

Superconductor-Insulator Quantum Phase Transition in Disordered FeSe Thin Films

R. Schneider,^{1,*} A. G. Zaitsev,¹ D. Fuchs,¹ and H. v. Löhneysen^{1,2}

¹*Institut für Festkörperphysik, Karlsruher Institut für Technologie, D-76021 Karlsruhe, Germany*

²*Physikalisches Institut, Karlsruher Institut für Technologie, D-76131 Karlsruhe, Germany*

(Received 30 January 2012; published 20 June 2012)

The evolution of two-dimensional electronic transport with increasing disorder in epitaxial FeSe thin films is studied. Disorder is generated by reducing the film thickness. The extreme sensitivity of the films to disorder results in a superconductor-insulator transition. The finite-size scaling analysis in the critical regime based on the Bose-glass model strongly supports the idea of a continuous quantum phase transition. The obtained value for the critical-exponent product of approximately $7/3$ suggests that the transition is governed by quantum percolation. Finite-size scaling with the same critical-exponent product is also substantiated when the superconductor-insulator transition is tuned with an applied magnetic field.

DOI: [10.1103/PhysRevLett.108.257003](https://doi.org/10.1103/PhysRevLett.108.257003)

PACS numbers: 74.70.Xa, 74.40.Kb, 74.62.En, 74.78.-w

Many different material systems undergo a superconductor-insulator transition (SIT) in the limit of two dimensions (2D) and zero temperature ($T = 0$) by the variation of a tuning parameter such as disorder, an applied magnetic field, or charge density [1–11]. Theoretical approaches to explain SITs have to deal with the question of how superconductivity disappears with increasing disorder. Here the interplay of the attractive and repulsive electron-electron interactions plays a crucial role. In the theory of boson localization [12] (also dirty-boson or Bose-glass model), a continuous SIT is predicted at $T = 0$ as a result of the competition between quantum phase fluctuations and long-range Coulomb repulsion. The prediction of the SIT as a continuous quantum phase transition (QPT) [13] by the bosonic model is particularly intriguing. The quantum fluctuations affect physical quantities at nonzero temperatures opening a route for the experimental study of QPTs. To evaluate measurements at $T \neq 0$ in the critical regime, finite-size scaling [12] is used, as described below. Scaling renders possible the determination of the critical exponents and, hence, the universality class of the transition. For instance, a value of the correlation-length exponent ν of $7/3$ is typical for the universality class of quantum percolation transitions [14]. As an additional signature, the bosonic model suggests a universal value of the critical sheet resistance equal to the quantum resistance for electron pairs $R_q = h/4e^2 \approx 6.45 \text{ k}\Omega$ (h : Planck constant, e : elementary charge).

Among the unconventional Fe-based superconductors, β -FeSe is the simplest one with respect to its chemical composition and crystal structure. The compound has an ambient-pressure transition temperature T_c of $\approx 8 \text{ K}$ [15]. The tetragonal PbO-type crystal structure consists of a stacking of parallel sheets with a distance of the c -axis lattice constant $c = 0.55 \text{ nm}$. This layered structure, together with a significant resistivity anisotropy of 1 order of magnitude to 2 orders of magnitude perpendicular and parallel to the sheets, make the compound inherently an

appropriate candidate for the study of 2D electronic transport in single crystals or thin films with their crystallographic c -axis perpendicular to the substrate plane.

In this study the evolution of the temperature-dependent sheet resistance with increasing disorder in c -axis oriented FeSe thin films is reported. Disorder is induced by decreasing the thickness of identically prepared nearly stoichiometric films. At critical values of the thickness and sheet resistance, a transition from the superconducting to the insulating state is observed. Finite-size scaling analysis in the critical regime according to the Bose-glass model reveals a critical-exponent product consistent with the prediction of a quantum percolation transition. These findings are independently confirmed when the SIT is tuned with an applied magnetic field.

The thin films were deposited onto single-crystalline (001)-oriented MgO substrates by radio-frequency sputtering of a sintered FeSe target. The temperature of the substrates was kept constant at nominal 480°C during deposition. The composition of the films was routinely inspected by Rutherford backscattering spectrometry. X-ray diffraction measurements revealed that the films grew in the tetragonal β phase with a strong c -axis texture irrespective of the film thickness. The thickness t of the films was varied over a wide range from nominally 1 nm to 1622 nm . All the films were prepared under otherwise identical sputtering conditions. Thickness measurements were usually performed using a stylus profiler or Rutherford backscattering spectrometry. The as-deposited films were patterned to stripes of length $l = 2 \text{ mm}$ and width $w = 0.6 \text{ mm}$. The direct-current resistance measurements were carried out between 1.2 K and room temperature. The resistance of one sample was also measured in an applied magnetic field ranging from 1 to 14 T perpendicular to the film plane. The measurement currents were between 0.1 and $10 \mu\text{A}$ and well within the linear region of the current-voltage characteristic. The appropriate quantity for the description of two-dimensional electronic

transport is the sheet resistance R_s in place of the resistivity ρ which characterizes transport in three dimensions. Therefore, the measured resistance R was converted to $R_s = Rwt/lc = \rho/c$ which is the sheet resistance R_s per Fe-Se sheet. R_s is material specific and represents a resistive quantity averaged over a number $N = t/c + 1$ of parallel-connected Fe-Se sheets in a c -axis oriented FeSe film of thickness t . Because of the resistivity anisotropy perpendicular and parallel to the sheets they are electrically decoupled to a great extent, and therefore the use of the sheet resistance per Fe-Se sheet appears to be justified.

Figure 1(a) shows the resistivity ρ_0 at $T = 0$ on the left-hand linear scale as a function of the film thickness on a log scale. From the maximum obtainable thickness of 1622 nm which was limited by peeling-off of the film, ρ_0 remains nearly constant down to 342 nm. In this thickness range the films exhibit bulklike features [16]. However, below a threshold of 300 nm, ρ_0 increases nearly linearly with decreasing $\log t$. The same thickness-threshold behavior also appears in the residual resistivity ratio $\text{RRR} = \rho(300 \text{ K})/\rho_0$ shown on the right-hand linear scale in Fig. 1(a). Figure 1(b) demonstrates the thickness-dependent $T_c(t)$ midpoint together with the 10%-to-90% transition width (bars). Starting with the thickest film, T_c slightly decreases from a remarkably high value of 10.9 K which may be due to an annealing effect during the long deposition time of 50 min, levels out at 8.6 K between 500 and 300 nm, and steeply drops for $t < 300$ nm. The dashed line is a Cooper-law fit, $T_c \propto \exp(-t^{-1})$, which is commonly used to fit experimental T_c data in thin films [17]. It

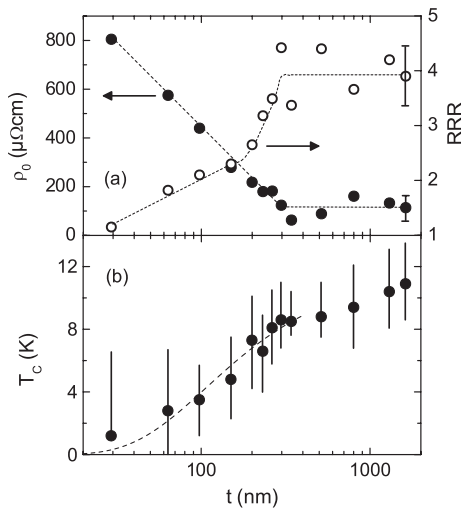


FIG. 1. (a) Variation of the resistivity ρ_0 at $T = 0$ (left-hand scale) and the residual resistivity ratio RRR (right-hand scale) with the film thickness t on a log scale. The dashed lines are guides to the eye. The bars indicate the spread of the data in the saturation region above 300 nm. (b) Dependence of the resistive midpoint T_c on t . The bars represent the 10%-to-90% transition widths. The dashed line is a Cooper-law fit to the data points below 300 nm.

is remarkable that our FeSe films show a threshold for ρ_0 and RRR, both quantifications of the strength of disorder, and for T_c already at a large thickness of 300 nm. This observation reveals a very high sensitivity to disorder mainly induced by decreasing the film thickness.

R_s is plotted in Fig. 2 versus the temperature T with the film thickness as a parameter. t extends from 1300 nm (bottom curve *a*) to nominally 1 nm (top curve *l*). For $t > 300$ nm (curves *a* and *b*), $R_s(T, t)$ behaves like a metal in the normal state. The zero-resistance state, $R_s(T_{c0}) = 0$ (within our resistance resolution of $\approx 10^{-4} \Omega$), is achieved at T_{c0} values from 4.4 to 6.6 K. For $t < 300$ nm (the thickness threshold found in Fig. 1) the curves *c* to *h* end at a finite resistance at the lowest measurement temperature of 1.2 K. Even the extrapolation to $T = 0$ does not result in a $R_s(0) = 0$ state. $R_s(0)$ increases over three decades with the thickness decreasing from 263 to 20 nm. The finite resistance is accompanied by the evolution of pronounced resistance tails becoming broader with smaller thickness. Their temperature dependence can be well fitted by an inverse Arrhenius law, $R_s(T) \propto \exp(T/T_0)$ with a constant T_0 , which is typically used to describe the sheet resistance of disordered granular superconductors below T_c [18]. Granularity means superconducting grains embedded in an insulating matrix. Electronic transport between neighboring grains is enabled either by Josephson tunneling via weak links or by quasiparticle tunneling. The importance of weak links in our FeSe films thinner than 300 nm is also evidenced by strong nonlinearities in the measured current-voltage characteristics over a three-decade current range above small critical currents of $\approx 10^{-5}$ to 10^{-4} A, reflecting a current-dependent sheet

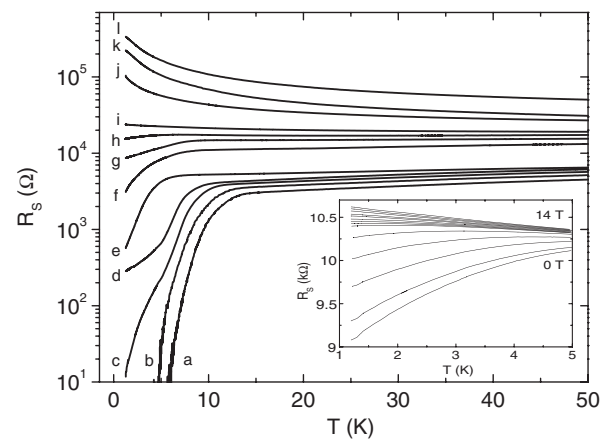


FIG. 2. Temperature dependence of the sheet resistance R_s per Fe-Se sheet with the mean film thickness t as a parameter. The curves are labeled from bottom to top by *a* to *l* corresponding to $t = 1300, 800, 263, 95, 80, 64, 29, 20, 19, 10, 2,$ and 1 nm, respectively. The inset shows $R_s(B, T)$ with an applied magnetic field B perpendicular to the plane of a 30 nm thick film as the tuning parameter. The values of B are 0, 1, 3, 5, 7, 8.5, 8.9, 9.3, 9.8, 10.5, 11, 12, 13, and 14 T (from bottom to top).

resistance and a broad critical-current distribution in the weak-link network. Thermal and quantum phase fluctuations in the superconducting order parameter are suggested as an explanation for the exponential R_s decrease at low temperatures and the finite resistance at $T = 0$, respectively [18,19]. Therefore, the FeSe films thinner than 300 nm can be categorized as crystalline epitaxial films, with features in their electronic transport characteristics that are typical for granularity. The appearance of such features in addition to the thickness dependence of T_c which is characteristic for epitaxial films might reflect the existence of two different intrinsic length scales which are sampled in the approach to a QPT. The presence of granularity is very compatible with the idea of quantum percolation which will be discussed below. At a thickness of 20 nm (curve *i*) $R_s(T)$ becomes insulatorlike with a negative temperature coefficient. Hence, there must be a critical value t_c of the thickness where R_s takes a temperature-independent critical value R_c that separates the superconducting and insulating branches of this direct SIT; i.e., intermediate metallic phases or resistance saturation at the lowest temperatures, as reported in [20], are not observed. In addition, $R_s(B, T)$ of a 30 nm thick film was measured with a perpendicular magnetic field B as the tuning parameter. The inset of Fig. 2 manifests a magnetic-field driven SIT which will be discussed further below.

The determination of t_c and R_c is demonstrated in the inset of Fig. 3. Isotherms of R_s from 2 to 8 K in steps of 2 K are plotted against t . Their intersection point, at which R_s

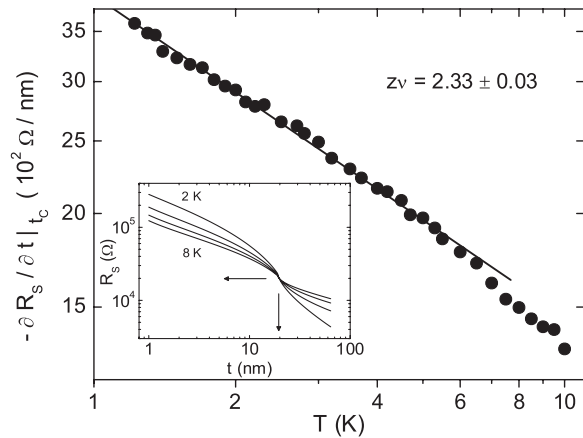


FIG. 3. Finite-size scaling analysis at nonzero temperatures of the negative film-thickness derivative of the sheet resistance R_s per Fe-Se sheet, $-\partial R_s/\partial t$, evaluated at the critical thickness t_c for $T < 10$ K on a log-log scale. The solid line up to 6.5 K is a linear least-square fit. Its slope gives an exponent product $z\nu = 2.33 \pm 0.03$. The inset shows the thickness dependence of R_s for temperatures of 2, 4, 6, and 8 K. The plot serves to determine the critical thickness $t_c = 19.5$ nm (vertical arrow) and the critical resistance $R_c = 19.8$ k Ω (horizontal arrow). Below t_c , R_s decreases with increasing temperature (insulating regime). Above t_c , R_s increases with increasing temperature (metallic regime).

does not depend on T , reveals values of $t_c = 19.5$ nm and $R_c = 19.8$ k Ω , as indicated by the vertical and horizontal arrows, respectively. R_c is approximately 3 times larger than R_q . Experimentally, R_c values different from R_q have been published by Yazdani *et al.* [6] and Marković *et al.* [2] for a number of thin-film materials, although there are also investigations by Steiner *et al.* [21] revealing R_c close to R_q . In all, R_c values ranging from approximately 0.5 to $3R_q$ were found experimentally. Thus, Gantmakher and Dolgoplov [13] concluded that the universality of R_c is confirmed so far only to an order of magnitude or that there is even no universal R_c for all material systems. The results probably depend on the quality of the samples. In our case of epitaxial thin films, the dimensionality could deviate from two due to a low electrical anisotropy perpendicular and parallel to the Fe-Se sheets enabling interplane electronic conduction. Unpaired normal electrons (fermionic excitations) are also suggested by Yazdani *et al.* [6] to contribute to the conduction and to obscure the universality of the Cooper-pair conduction. Theoretically, the critical resistance is a nonuniversal constant, if no perfect duality between Cooper pairs (charge) and vortices and a more realistic interaction between charges are assumed [1].

The finite-size scaling dependence of R_s on T and a tuning parameter x in two dimensions has the form $R_s(x, T) = R_c f(|x - x_c|/T^{1/z\nu})$ [12]. x can be the film thickness as a measure of disorder, magnetic field, or charge density. $|x - x_c| = \delta$ is called the control parameter, where x_c is the critical tuning parameter. The quantum mechanical ground state of a system changes when x crosses the critical value x_c . R_c is the critical sheet resistance, and f is an arbitrary function with $f(0) = 1$. The exponent product $z\nu$ comprises the correlation-length exponent ν and the dynamical critical exponent z , which are defined via $\xi \sim |\delta|^{-\nu}$ and $\xi_\tau \sim \xi^z \sim |\delta|^{-z\nu}$. ξ and ξ_τ are the spatial and the temporal correlation lengths, respectively, which diverge near a QPT. The term “finite size” refers to the finite scaling variable $\delta/T^{1/z\nu} \propto (L_\phi/\xi)^{1/\nu}$. At finite temperature the divergence of the correlation length ξ is cut off by the dephasing length L_ϕ which is bounded by the temperature: $\xi \propto L_\phi \propto T^{-1/z}$.

To obtain the exponent product $z\nu$, we consider the film-thickness derivative of $R_s(t)$ taken at the critical thickness t_c , since $\log(-\partial R_s/\partial t)|_{t_c} = -(1/z\nu)\log T + \text{const}$ according to Hebard *et al.* [6] and Seidler *et al.* [8]. If the experimental R_s values obey finite-size scaling, a log-log plot of $-\partial R_s/\partial t|_{t_c}$ versus T gives a straight line with a slope equal to $-1/z\nu$. This is demonstrated in the main frame of Fig. 3 for our FeSe data in the vicinity of the critical thickness (see inset). The plot is linear up to 6.5 K and reveals an exponent product $z\nu = 2.33 \pm 0.03$. The deviation from the scaling behavior above 6.5 K may be due to quadratic finite-temperature corrections neglected in the above $R_s(t, T)$ scaling law, or the data may fall outside the critical regime whose width is unknown.

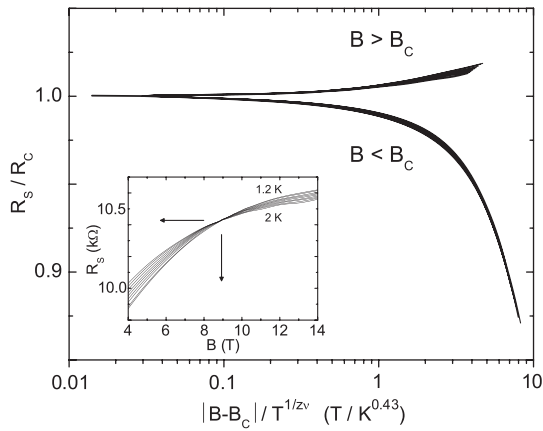


FIG. 4. $R_s(B, T)$ (cf. inset of Fig. 2) normalized to the critical value R_c versus the magnetic-field scaling variable $|B - B_c|/T^{1/z\nu}$ ($B_c = 8.92$ T, $z\nu = 2.33$) for 9 temperatures between 1.2 and 2 K, and 29 values of the magnetic field from 0 to 14 T. The lower and upper branches take into account the change in sign of $B - B_c$ and are identified with $B < B_c$ and $B > B_c$, respectively. The intersection point of the isotherms between 1.2 and 2 K in steps of 0.1 K in the inset reveals the critical values of $B_c = 8.92$ T (vertical arrow) and $R_c = 10.4$ k Ω (horizontal arrow)

To test the scaling form in a second independent way, the $R_s(B, T)$ measurements in the inset of Fig. 2 are used. An Arrhenius plot, i.e., $\ln R_s$ versus $1/T$, for B below the critical field B_c reveals a linear behavior with a finite slope that turns to zero for B close to B_c , down to a magnetic-field dependent limiting temperature, for instance 2.6 K for $B = 0$ and 1.5 K for $B = 5$ T, respectively. This result in the high-temperature region indicates the thermally activated motion of vortices with an activation energy that decreases with increasing magnetic field. Below the limiting temperature, R_s flattens with decreasing temperature and shows a trend to saturation. Such a feature might be typical for the occurrence of an intervening metallic state in an indirect magnetic-field driven SIT [3]. A metallic phase would imply that the SIT is actually a metal-insulator transition. Nevertheless, the superconductor-insulator scaling theory [12] describes our magnetoresistance data very well, as demonstrated below. For intermediate field strengths, scaling behavior at higher temperature is often observed in conjunction with metallic behavior at low temperature according to Kapitulnik *et al.* [14]. These temperature and magnetic-field conditions may define an asymptotic limit for the finite-size scaling theory. The issue of an intermediate metallic regime is an open question in the research field of SIT [1] and requires further experimental and theoretical studies. In Fig. 4, $R_s(B, T)$ normalized to the critical value R_c is plotted against the magnetic-field scaling variable $|B - B_c|/T^{1/z\nu}$ without the use of fitting parameters. B_c is determined by the intersection point of $R_s(B, T = \text{const})$ isotherms and amounts to 8.92 T, as shown in the inset of

Fig. 4. The critical resistance R_c amounts to 10.4 k Ω which is $\approx 1.6R_q$ and hence half the critical value of the thickness-driven SIT (cf. inset in Fig. 3). The deviation from R_q is not surprising after the above discussion on this topic. The difference between the magnetic-field and thickness related R_c indicates a possible thickness dependence of R_c in a magnetic field for FeSe which deserves further investigation. Such a dependence was already found in amorphous Bi and Be [22]. For $z\nu = 2.33$ the two branches $B < B_c$ and $B > B_c$ collapse onto a single cusplike curve each when B approaches B_c . This result additionally confirms the scaling prediction of the Bose-glass model with a value of 2.33 for the critical-exponent product. A value of $z = 1$ is predicted for disordered systems of charged bosons where long-range Coulomb interactions are favored [23], and has been experimentally verified for two-dimensional amorphous InO $_x$ and MoGe films [6]. Assuming $z = 1$, $\nu = 2.33 \approx 7/3$ is the correlation-length exponent of anisotropic disordered two-dimensional systems with a metal-insulator transition [24]. The value is consistent with the prediction of the quantum percolation model for the SIT and the quantum Hall effect [14,21] suggesting that the observed SIT in the disordered FeSe films is a quantum rather than a classical percolation transition with $\nu = 4/3$.

In summary, the successful finite-size scaling analysis supports the bosonic description of the disorder and magnetic-field driven SIT in epitaxial FeSe thin films. The critical sheet resistance, however, does not meet the supposed universal quantum resistance for electron pairs, thus challenging its universality. Our analysis also implies the two-dimensional character of the electronic transport in the anisotropic compound. The critical-exponent product points to quantum percolation underlining the importance of weak links in the films.

*rudolf.schneider2@kit.edu

- [1] For a review, see A. M. Goldman and N. Marković, *Phys. Today* **51**, No. 11 39 (1998); A. M. Goldman, in *BCS: 50 Years*, edited by L. N. Cooper and D. Feldman (World Scientific, Singapore, 2011).
- [2] H. M. Jaeger, D. B. Haviland, B. G. Orr, and A. M. Goldman, *Phys. Rev. B* **40**, 182 (1989); N. Marković, A. M. Mack, G. Martinez-Arizala, C. Christiansen, and A. M. Goldman, *Phys. Rev. Lett.* **81**, 701 (1998); A. Frydman, O. Naaman, and R. C. Dynes, *Phys. Rev. B* **66**, 052509 (2002).
- [3] Y. Qin, C. L. Vicente, and J. Yoon, *Phys. Rev. B* **73**, 100505(R) (2006).
- [4] S. J. Lee and J. B. Ketterson, *Phys. Rev. Lett.* **64**, 3078 (1990).
- [5] T. Wang, K. M. Beauchamp, D. D. Berkley, B. R. Johnson, J.-X. Liu, J. Zhang, and A. M. Goldman, *Phys. Rev. B* **43**, 8623 (1991); S. Tanda, S. Ohzeki, and T. Nakayama, *Phys. Rev. Lett.* **69**, 530 (1992); M. Inoue, H. Matsushita,

- H. Hayakawa, and K. Ohbayashi, *Phys. Rev. B* **51**, 15 448 (1995).
- [6] A. F. Hebard and M. A. Paalanen, *Phys. Rev. Lett.* **65**, 927 (1990); A. Yazdani and A. Kapitulnik, *Phys. Rev. Lett.* **74**, 3037 (1995); Y.-H. Lin and A. M. Goldman, *Phys. Rev. Lett.* **106**, 127003 (2011).
- [7] T. I. Baturina, C. Strunk, M. R. Baklanov, and A. Satta, *Phys. Rev. Lett.* **98**, 127003 (2007).
- [8] G. T. Seidler, T. F. Rosenbaum, and B. W. Veal, *Phys. Rev. B* **45**, 10 162 (1992).
- [9] K. A. Parendo, K. H. Sarwa, B. Tan, A. Bhattacharya, M. Eblen-Zayas, N. E. Staley, and A. M. Goldman, *Phys. Rev. Lett.* **94**, 197004 (2005).
- [10] A. T. Bollinger, G. Dubuis, J. Yoon, D. Pavuna, J. Misewich, and I. Božović, *Nature (London)* **472**, 458 (2011).
- [11] X. Leng, J. Garcia-Barriocanal, S. Bose, Y. Lee, and A. M. Goldman, *Phys. Rev. Lett.* **107**, 027001 (2011).
- [12] M. P. A. Fisher, *Phys. Rev. Lett.* **65**, 923 (1990); M. P. A. Fisher, G. Grinstein, and S. M. Girvin, *Phys. Rev. Lett.* **64**, 587 (1990); M.-C. Cha, M. P. A. Fisher, S. M. Girvin, M. Wallin, and A. P. Young, *Phys. Rev. B* **44**, 6883 (1991).
- [13] S. L. Sondhi, S. M. Girvin, J. P. Carini, and D. Shahar, *Rev. Mod. Phys.* **69**, 315 (1997); S. Sachdev, *Quantum Phase Transitions* (Cambridge University Press, Cambridge, England, 1999); V. F. Gantmakher and V. T. Dolgoplov, *Phys. Usp.* **53**, 1 (2010).
- [14] D.-H. Lee, Z. Wang, and S. Kivelson, *Phys. Rev. Lett.* **70**, 4130 (1993); A. Kapitulnik, N. Mason, S. A. Kivelson, and S. Chakravarty, *Phys. Rev. B* **63**, 125322 (2001); Y. Dubi, Y. Meir, and Y. Avishai, *Phys. Rev. Lett.* **94**, 156406 (2005).
- [15] F.-C. Hsu *et al.*, *Proc. Natl. Acad. Sci. U.S.A.* **105**, 14 262 (2008); S. Medvedev *et al.*, *Nature Mater.* **8**, 630 (2009).
- [16] S.-G. Jung, N.H. Lee, E.-M. Choi, W.N. Kang, S.-I. Lee, T.-J. Hwang, and D. H. Kim, *Physica (Amsterdam)* **470C**, 1977 (2010).
- [17] L. N. Cooper, *Phys. Rev. Lett.* **6**, 689 (1961); S. A. Wolf, J. J. Kennedy, and M. Nisenoff, *J. Vac. Sci. Technol.* **13**, 145 (1976); J. Simonin, *Phys. Rev. B* **33**, 7830 (1986).
- [18] Y. M. Strel'niker, A. Frydman, and S. Havlin, *Phys. Rev. B* **76**, 224528 (2007); A. Frydman, O. Naaman, and R. C. Dynes, *Phys. Rev. B* **66**, 052509 (2002).
- [19] L. Merchant, J. Ostrick, R. P. Barber, Jr., and R. C. Dynes, *Phys. Rev. B* **63**, 134508 (2001).
- [20] Y. Seo, Y. Qin, C. L. Vicente, K. S. Choi, and J. Yoon, *Phys. Rev. Lett.* **97**, 057005 (2006); N. Mason and A. Kapitulnik, *Phys. Rev. Lett.* **82**, 5341 (1999).
- [21] M. Steiner, N. P. Breznay, and A. Kapitulnik, *Phys. Rev. B* **77**, 212501 (2008).
- [22] N. Marković, C. Christiansen, A. M. Mack, W. H. Huber, and A. M. Goldman, *Phys. Rev. B* **60**, 4320 (1999); E. Bielejec and W. Wu, *Phys. Rev. Lett.* **88**, 206802 (2002).
- [23] I. F. Herbut, *Phys. Rev. Lett.* **87**, 137004 (2001).
- [24] M. Rühländer and C. M. Soukoulis, *Phys. Rev. B* **63**, 085103 (2001).